

- patients with Parkinson's disease with or without dementia. *Ann Nuklearmedizin* 1992;6:241-246.
37. Benson DF, Kuhl DE, Hawkins RA, Phelps ME, Cummings JL, Tsai SY. The fluorodeoxyglucose ¹⁸F scan in Alzheimer's disease and multi-infarct dementia. *Arch Neurol* 1983;40:711-714.
 38. Kuhl DE, Metter EJ, Benson DF, et al. Similarities of cerebral glucose metabolism in Alzheimer's and Parkinson's dementia. *J Cereb Blood Flow Metab* 1985;5:S169-S170.
 39. Liu RS, Lin KN, Wang SJ, et al. Cognition and ^{99m}Tc-HMPAO SPECT in Parkinson's disease. *Nucl Med Commun* 1992;13:744-748.
 40. Eberling JL, Richardson BC, Reed BR, Wolfe N, Jagust WJ. Cortical glucose metabolism in Parkinson's disease without dementia. *Neurobiol Aging* 1994;15:329-335.
 41. Rougemont D, Baron JC, Collard P, Bustany P, Comar D, Agid Y. Local cerebral glucose utilization in treated and untreated patients with Parkinson's disease. *J Neurol Neurosurg Psychiatry* 1984;47:824-830.
 42. Bodis-Wollner I, Yahr MD. Measurements of visual evoked potentials in Parkinson's disease. *Brain* 1978;101:661-671.
 43. Bodis-Wollner I, Yahr MD, Mylin L, Thornton J. Dopaminergic deficiency and delayed visual evoked potentials in humans. *Ann Neurol* 1982;11:478-483.
 44. Ikeda H, Head GM, Ellis CJ. Electrophysiological signs of retinal dopamine deficiency in recently diagnosed Parkinson's disease and a follow up study. *Vision Res* 1994;34:2629-2638.
 45. Nguyen-Legros J, Harnois C, Di Paolo T, Simon A. The retinal dopamine system in Parkinson's disease. *Clin Vision Sci* 1993;8:1-12.
 46. O'Mahony D, Rowan M, Feely J, O'Neill D, Walsh JB, Coakley D. Parkinson's dementia and Alzheimer's dementia: an evoked potential comparison. *Gerontology* 1993;39:228-240.
 47. Braak H, Braak E. Neuropathological staging of Alzheimer-related changes. *Acta Neuropathol (Berl)* 1991;82:239-259.
 48. Jagust WJ, Eberling JL, Richardson BC, et al. The cortical topography of temporal lobe hypometabolism in early Alzheimer's disease. *Brain Res* 1993;629:189-198.
 49. Ince P, Irving D, MacArthur F, Perry RH. Quantitative neuropathological study of Alzheimer-type pathology in the hippocampus: comparison of senile dementia of Alzheimer type, senile dementia of Lewy body type, Parkinson's disease and non-demented elderly control patients. *J Neurol Sci* 1991;106:142-152.
 50. Hansen LA, Masliah E, Quijada-Fawcett S, Rexin D. Entorhinal neurofibrillary tangles in Alzheimer disease with Lewy bodies. *Neurosci Lett* 1991;129:269-272.
 51. Lippa CF, Smith TW, Swearer JM. Alzheimer's disease and Lewy body disease: a comparative clinicopathological study. *Ann Neurol* 1994;35:81-88.
 52. Wakabayashi K, Honer WG, Masliah E. Synapse alterations in the hippocampal-entorhinal formation in Alzheimer's disease with and without Lewy body disease. *Brain Res* 1994;667:24-32.
 53. Katzman R, Galasko D, Saitoh T, Thal LJ, Hansen L. Genetic evidence that the Lewy body variant is indeed a phenotypic variant of Alzheimer's disease. *Brain Cogn* 1995;28:259-265.

Fluorine-18-FDG PET and Iodine-123-IMT SPECT in the Evaluation of Brain Tumors

Wolfgang Weber, Peter Bartenstein, Markus W. Gross, Dieter Kinzel, Hans Daschner, Horst J. Feldmann, Günther Reidel, Sibylle I. Ziegler, Christiano Lumenta, Michael Molls and Markus Schwaiger
Departments of Nuclear Medicine and Radiation Oncology, Klinikum Rechts der Isar; and Department of Neurosurgery Krankenhaus München-Bogenhausen, Technical University of Munich, Munich, Germany

The high glucose utilization of normal gray matter limits the detection of brain tumor tissue by PET using ¹⁸F-fluorodeoxyglucose (FDG). The aim of this study was to evaluate whether the examination of amino acid transport with the SPECT tracer ¹²³I-alpha-methyl-L-tyrosine (IMT) allows better identification of tumor tissue than FDG-PET. **Methods:** Nineteen patients (16 with gliomas, 3 with nontumorous lesions) were included in the study. Two independent observers classified PET and SPECT images as positive or negative for tumor tissue and defined the extent of tumor with regions of interest. Tracer uptake of FDG and IMT was quantified by calculating the tumor uptake relative to contralateral gray and white matter. **Results:** SPECT studies were interpreted concordantly in 18 patients ($\kappa = 0.77$) and all tumors were identified by both observers. PET studies were interpreted discordantly in 4 patients ($\kappa = 0.52$) and only 10 tumors were identified by both observers. Interobserver variability in definition of tumor extent was significantly lower in the IMT-SPECT than in the FDG-PET studies ($p = 0.03$). Mean tumor uptake relative to gray and white matter was 1.93 ± 0.42 and 2.25 ± 0.46 for IMT and 0.93 ± 0.32 and 1.61 ± 0.52 for FDG. All tumor uptake ratios were significantly ($p < 0.01$) higher for IMT than FDG, even when only glioblastomas were analyzed. No significant correlation was observed between the various uptake ratios of FDG and IMT. **Conclusion:** Despite the lower resolution and lower sensitivity of SPECT compared with PET, IMT-SPECT was clearly superior to FDG-PET in the detection and delineation of tumor tissue.

Key Words: fluorine-18-FDG; iodine-123-IMT; gliomas

J Nucl Med 1997; 38:802-806

Aggressive neurosurgery, radiotherapy and chemotherapy are the standard of care for most patients with primary brain tumors (1). These combined therapeutic strategies can lead to considerable side effects (2) and achieve long-term survival only in a small percentage of patients (3). Therefore, reliable recognition of viable tumor tissue and measurement of treatment effect are of great importance. Several studies have demonstrated that CT and MRI cannot reliably differentiate viable tumor tissue from tumor-associated edema, postoperative changes or radiation necrosis (4). Therefore, imaging methods that are based on specific markers of tumor tissue and metabolism have been proposed as alternatives to these techniques. Since 1982, PET using the glucose analog ¹⁸F-fluor-deoxy-D-glucose (FDG) has been applied for noninvasive tumor grading, differentiation of tumor recurrence from radiation necrosis and determination of prognosis (5-8). However, the high glucose utilization of gray matter complicates the identification of tumor tissue by FDG-PET (9-11). Therefore, difficulties in the visual interpretation of FDG-PET studies and the quantification of FDG uptake were reported (9,11). As protein synthesis rate of normal brain tissue is several degrees of magnitude lower than its glucose utilization [about 0.5 nmol/g/min for leucine versus 0.3 μ mol/100 g/min for glucose (12)], amino acid tracers have been proposed as an alternative to FDG in the metabolic characterization of brain tumors (13).

Iodine-123-alpha-methyl-L-tyrosine (IMT) is an amino acid analog initially developed for imaging melanomas and the adrenal medulla (14). IMT has a similar affinity to the neutral amino acid carrier at the blood-brain barrier as L-tyrosine but is not further metabolized and not incorporated into proteins (15,16). Its uptake in brain tumors can be saturated by natural amino acids, indicating that IMT uptake in these tumors is due

Received Jun. 9, 1996; revision accepted Dec. 20, 1996.

For correspondence or reprints contact: Wolfgang Weber, MD, Department of Nuclear Medicine, Klinikum rechts der Isar, Technical University of Munich, Ismaningerstrasse 22, D-81675 Munich, Germany.

to a specific amino-acid transport system (17). So far this tracer has been shown to accumulate intensively in brain tumors of different histologic types and grading, while the uptake in normal brain is low (15,18). In consideration of these results, IMT appears to be a promising new agent for metabolic imaging of brain tumors with SPECT. SPECT cameras for ^{123}I -labeled tracers are, however, clearly inferior in terms of sensitivity and resolution compared with current PET scanners. It is unknown whether IMT-SPECT is superior to FDG-PET in the detection and delineation of brain tumors. Therefore, the aim of this study was to compare these two techniques in a series of patients with suspected primary or recurrent brain tumors to determine:

1. What is the contrast between normal brain and tumor tissue in IMT-SPECT compared to FDG-PET?
2. Is the delineation of brain tumors from normal tissue more reliable with IMT-SPECT than with FDG-PET?
3. What is the correlation between IMT and FDG uptake in brain tumors?

METHODS

Patients

We studied patients who were referred from the departments of radiotherapy and neurosurgery for an FDG-PET study because of suspected recurrent tumor, differential diagnosis of intracerebral lesions or determination of residual disease after debulking surgery. An MR examination, including T1- and T2-weighted sequences and T1-weighted sequences after administration of Gd-DTPA, had to have been performed previously and interpreted as compatible with tumor. FDG-PET and IMT-SPECT were performed within 2 wk after the MR study. Exclusion criteria were pregnancy and inability to give informed consent. Details of the study were explained to the patients by a physician. The study was approved by the university's ethics committee.

Data Acquisition

FDG was produced by a standard technique of nucleophilic fluorination (19). PET examinations were performed on fasted patients in a room with dimmed light, no conversation and low ambient noise, primarily from the scanner gantry fans. The PET tomograph had axial and transaxial resolutions, at FWHM, of about 5 and 8 mm, respectively. A 20-min static acquisition was performed starting 40 min after injection of 270–370 MBq FDG. Attenuation was corrected with the standard separate ellipse algorithm provided in the scanner software. Images were reconstructed by filtered backprojection using a Hanning filter with a cutoff frequency of 0.8 Nyquist. The image pixel counts were calibrated to activity concentrations (Bq/g), and standardized uptake values (SUV) were calculated using the formula:

$$\text{SUV} =$$

$$(\text{tissue concentration [Bq/g]})/(\text{injected dose [Bq]}/\text{body weight [g]}).$$

IMT labeled with ^{123}I by direct electrophilic iodination using Iodogen as an oxidant (20). Radiochemical yields were about 80% and specific activities of approximately 160 TBq/mmol were achieved. Patients were examined by IMT-SPECT after fasting for at least 4 hr. The patients received 900 mg sodium perchlorate before the IMT injection to minimize radioactive iodide uptake by the thyroid. Data acquisition was started 30 min after intravenous injection of 185–370 MBq IMT. Images ($n = 120$) of 45 sec duration were acquired with a triple-head camera equipped with a dedicated ^{123}I collimator (collimator thickness 60 mm, septal thickness 0.5 mm) (21). With this collimator, the camera provides an axial and transaxial resolution of about 11 mm FWHM. Images

were reconstructed by filtered back-projection using a Butterworth filter (10. order, cutoff frequency 0.4 Nyquist).

Visual Image Interpretation

For visual analysis of the PET studies, SUV images were displayed on a computer monitor in the axial, coronal and sagittal orientations using an inverted gray scale with normalization of the images to a maximum SUV of 7.0. SPECT images were normalized to the maximum uptake in the study and displayed in the same way. Qualitative interpretation of PET and SPECT images was performed by two independent observers (PB and HD) blinded to the clinical data of the patient. PET and SPECT studies were evaluated in conjunction with the corresponding MR images. Studies were classified as positive or negative for the presence of tumor tissue.

Quantitative Analysis

Regions of interest (ROIs) were placed manually over focal FDG or IMT accumulations at the site of maximum tracer accumulation by two observers (PB and WW). To determine the percentage of overlap between the tumor areas A_1 and A_2 defined by the two observers, the following parameter, I , was calculated:

$$I = \frac{(A_1 \cap A_2)}{(A_1 \cup A_2)}.$$

In addition, the mean tracer uptake values of ROIs A_1 and A_2 were compared to each other. For further analysis, a ROI was defined by consensus using the MR images as a reference. The maximum and mean tracer uptake in these ROIs were determined and ratios were calculated relative to the contralateral gray and white matter. Contralateral gray and white matter (semiovale center) were defined in consecutive slices in the PET and SPECT studies. MR images were used as a reference to avoid inclusion of the ventricular system in white matter ROIs and inclusion of white matter in the gray matter ROIs. The volume of the reference ROIs was at least 3 cm³.

Statistical Analysis

The interobserver variability in the qualitative evaluation of the PET and SPECT studies was evaluated by kappa statistics (22). Uptake ratios are presented as mean \pm s.d. The correlation between tumor grading and FDG or IMT uptake was analyzed by the Kruskal-Wallis test. Quantitative parameters obtained by the different imaging methods in individual patients were compared by a two-tailed, paired t-test and by Pearson's correlation coefficient. All statistical tests were performed at the 5% level of significance.

RESULTS

Nineteen consecutive patients (14 men, 5 women) were included into the study over an 11-mo period. Mean age was 54 yr (range 35–75 yr). Patient characteristics, tumor type, pre-treatment and mode of diagnosis are summarized in Table 1. Overall, 16 primary brain tumors and 3 nontumorous lesions were studied. Ten patients were imaged for differential diagnosis of intracerebral lesions. These lesions were later confirmed by open surgery or stereotactic biopsy. Three patients were examined after debulking surgery for intracerebral tumors. Macroscopic residual tumor was demonstrated by early (within 48 hr) postoperative MRI. The interval between surgery and PET and SPECT imaging ranged between 1 and 4 wk. Six patients were imaged for suspected tumor recurrency. In four of these patients, recurrent tumors were verified by stereotactic biopsy. The remaining two patients (Patients 18 and 19) with suspected recurrent Grade II and III astrocytomas had negative PET and SPECT findings and were not operated on for ethical reasons. In these two patients, clinical follow-up for 6 mo in

TABLE 1
Clinical Data

Patient no.	Sex	Age (yr)	Histology	max Ø (cm)	Mode of diagnosis	Pretreatment
1	M	61	Glioblastoma	6.8	Biopsy	Surgery*
2	F	42	Astrocytoma II	4.9	Biopsy	None
3	M	57	Glioblastoma	5.3	Surgery	None
4	M	39	Mixed glioma II	7.5	Biopsy	None
5	M	60	Glioblastoma	5.7	Surgery	None
6	M	72	Glioblastoma	5.4	Surgery	None
7	M	54	Glioblastoma	5.0	Surgery	None
8	M	55	Glioblastoma	1.9	Surgery	Surgery†
9	M	53	Glioblastoma	7.0	Biopsy	None
10	F	37	Glioblastoma	5.5	Surgery	Surgery + radiotherapy*
11	F	75	Astrocytoma III	6.8	Biopsy	None
12	F	55	Astrocytoma III	3.6	Biopsy	None
13	M	46	Glioblastoma	1.5	Surgery	Surgery†
14	M	57	Glioblastoma	1.5	Biopsy	Surgery + radiotherapy*
15	F	49	Oligodendroglioma III	3.8	Biopsy	Surgery + radiotherapy*
16	M	60	Glioblastoma	1.8	Surgery	Surgery†
17	M	61	Hematoma	2.5	Surgery	None
18	M	61	n.a.	6.0	Follow-up	Surgery + ¹²⁵ I-seeds
19	M	35	n.a.	3.5	Follow-up	Surgery

*Recurrent tumor.

†Residual tumor after surgery.

Patient 18 and 3 mo in Patient 19 showed no signs of disease progression and a presumptive diagnosis of radiation necrosis and persistent postoperative edema was made.

Visual Image Interpretation

Eighteen of the 19 IMT studies were interpreted concordantly by the two observers. There was disagreement only in one case of intracerebral hematoma that was considered by one observer to cause pathological IMT accumulation ($\kappa = 0.77$). All of the 16 histologically confirmed tumors were identified as focal IMT accumulations by both observers. Despite the lower resolution of the SPECT camera compared with the PET scanner, four small tumors with a diameter of less than 2 cm were clearly identified by IMT-SPECT. Two of these tumors were interpreted discordantly by the two observers on the FDG-PET images because they were adjacent to normal cortical structures (Table 2).

Fourteen of the 16 tumors were identified on the FDG-PET images by at least one of the two observers. However, only 10 tumors were identified by both observers. The two cases of presumptive radiation necrosis and postoperative edema were correctly identified by both observers, whereas the intracerebral hematoma was considered as positive for tumor by both observers. Two low-grade astrocytomas were not detected by either observer and two recurrent and two residual tumors after partial resection of a glioblastoma were not considered by one observer to cause pathologically increased FDG uptake (Table 2). Overall, the kappa value between the two observers was 0.52 (Table 2). As an example for the difficulties in the visual interpretation of FDG-PET, Figure 1 shows the PET and SPECT studies of a patient with a recurrent glioblastoma (Patient 10).

Regions of interest (ROIs) defined by the two observers in the IMT images showed a high correspondence. The mean value of the parameter I determining the overlap of the tumor areas was 0.76 ± 0.07 (Fig. 2). For FDG-PET, ROIs were only analyzed when both observers had identified pathological FDG

accumulations. The I value for these tumors was 0.55 ± 0.31 , thus being significantly ($p = 0.03$) lower than with IMT-SPECT (Fig. 2). The mean IMT uptake in the ROIs defined by the two observers showed a high correlation ($r = 0.999$, $p = 0.0001$, Fig. 3A). The correlation between mean FDG uptake showed considerable more scatter ($r = 0.84$, $p = 0.002$, Fig. 3B).

The values of the mean and maximum uptake ratios based on the consensus ROIs for IMT and FDG are shown in Table 2 and Figure 4. With FDG-PET, all tumors except a Grade II astrocytoma were hypermetabolic compared to normal white matter. Since uptake of normal gray matter was about twice the uptake of normal white matter, only four tumors (all glioblastomas) were hypermetabolic compared with normal gray matter. The mean SUV of the tumors was significantly higher than the mean SUV of the normal white matter ($p = 0.001$) but not significantly different from normal gray matter ($p = 0.188$). The results were similar when only glioblastomas were analyzed ($p = 0.002$ and $p = 0.73$, respectively).

With IMT, all tumors were hypermetabolic compared to normal white and gray matter. Due to the low uptake of IMT in normal gray matter, tumor-to-gray-matter ratios were only 17% lower than tumor-to-white-matter ratios. All uptake ratios were significantly ($p < 0.001$) higher for IMT than for FDG, even when only glioblastomas were analyzed ($p < 0.01$). The mean and maximum uptake ratios relative to white matter for IMT were 1.4-fold higher than for FDG. The mean and maximum uptake ratios relative to gray matter for IMT were 2.1-fold higher than for FDG.

For FDG, significant correlations between the maximum and mean tumor uptake and histological grading were found ($p = 0.015$ and $p = 0.029$). No significant correlation was found between any of the uptake ratios of IMT and the histological grading. Although a tendency for higher IMT uptake in tumors with high FDG uptake was observed, no significant correlation between any of the uptake ratios of FDG and IMT was found. As an example, the correlation between the maximum FDG and

TABLE 2
 IMT and FDG Uptake Relative to Normal White and Gray Matter

	Patient no.	IMT/WM		IMT/GM		FDG/WM		FDG/GM		Visual interpretation*	
		mean	max	mean	max	mean	max	mean	max	PET	SPECT
Brain tumors											
	1	2.59	3.28	2.00	2.53	2.22	2.71	1.49	1.81	p	p
	2	1.75	2.22	1.90	2.41	1.19	1.43	0.69	0.83	n	p
	3	2.61	3.54	2.53	3.44	2.18	2.57	1.53	1.81	p	p
	4	3.31	4.21	2.63	3.34	1.00	1.38	0.55	0.77	n	p
	5	2.42	2.93	1.87	2.27	2.13	2.65	1.37	1.71	p	p
	6	2.80	3.22	2.21	2.54	1.09	1.81	0.59	0.99	p	p
	7	1.68	2.18	1.44	1.86	1.37	1.70	0.82	1.02	p	p
	8	2.07	2.37	1.69	1.93	1.47	1.59	0.76	0.82	d	p
	9	2.74	3.84	2.65	3.71	2.01	2.59	1.05	1.36	p	p
	10	1.75	2.25	1.58	2.03	1.19	1.53	0.59	0.76	d	p
	11	1.85	2.40	1.37	1.78	1.34	1.83	0.67	0.91	p	p
	12	2.17	2.55	1.97	2.31	1.75	1.93	0.94	1.04	p	p
	13	2.25	2.76	2.17	2.66	1.59	1.81	0.96	1.09	p	p
	14	2.05	2.52	1.84	2.26	2.32	3.03	1.20	1.57	p	p
	15	1.83	2.42	1.43	1.88	1.38	1.70	0.66	0.82	d	p
	16	2.16	2.77	1.60	2.06	1.59	1.88	1.04	1.22	d	p
Mean		2.25	2.84	1.93	2.44	1.61	2.01	0.93	1.16		
s.d.		0.46	0.61	0.42	0.59	0.44	0.52	0.32	0.38		
Nontumorous lesions											
	17	1.69	2.05	1.43	1.73	1.84	2.34	0.89	1.13	p	d
	18	1.65	1.65	1.31	1.31	1.54	1.91	0.77	0.95	n	n
	19	1.06	1.88	0.91	1.61	1.38	2.06	0.66	0.98	n	n
Mean		1.47	1.86	1.22	1.55	1.59	2.10	0.77	1.02		
s.d.		0.35	0.20	0.27	0.22	0.23	0.22	0.12	0.10		

*Overall, the kappa for the agreement between the two observers is 0.77 for IMT-SPECT and 0.52 for FDG-PET. p = positive; n = negative; d = discordant study interpretation.

IMT uptake relative to white matter is shown in Figure 5 ($r = 0.29$, $p = 0.27$).

DISCUSSION

In this comparison of IMT-SPECT and FDG-PET imaging in the evaluation of intracerebral tumors, 16 consecutive gliomas showed a 2.1-fold higher mean tumor uptake of IMT than FDG relative to normal gray matter. The high tumor-to-background ratio with IMT-SPECT resulted in easy detection of all tumors and high correspondence in defining tumor extent by the two observers. FDG-PET images showed only low contrast between tumor tissue and normal gray matter. A limited consensus in the interpretation of FDG-PET studies by two observers was achieved. In cases where both a observers found pathological FDG accumulation, differences in the definition of tumor extent by a ROI were large.

The low uptake ratios of FDG in brain tumors in this study are in good agreement with the values reported by Debelke et al. (23) in a group of 38 gliomas. Difficulties in the qualitative and quantitative evaluation of brain tumors due to low contrast of FDG images have been reported by several authors since the introduction of the method (6,9,10). Quantification of tumor metabolism is hampered by the low contrast of FDG images in two ways: First, as shown in our study, interobserver variability in definition of ROIs for semiquantitative analysis is considerable. Second, spillover from normal cortical tissue may be a major source of the measured activity in the tumor. Because of the low uptake in normal brain, tracers of amino-acid metabolism may help to overcome these problems in the metabolic evaluation of brain tumors. In this study, we could demonstrate that IMT-SPECT allowed more reliable definition of tumor

extent and quantification of tracer uptake, although SPECT is principally inferior to PET with respect to image resolution and quantitative analysis.

Ishizu et al. (24) suggested increasing the contrast of brain tumors in FDG-PET studies by infusion of glucose to decrease FDG uptake in normal gray matter. In their study, the tumor-to-cortex ratio increased from 0.89 to 1.15 ($26 \pm 5.7\%$) in 10 patients with various intracranial tumors by rising the blood glucose level from 107 ± 19 to 242 ± 43 mg/dl. These data show that the contrast between gray matter and tumor tissue remains low, even with glucose loading. In addition, glucose loading further complicates the PET procedure since it requires intravenous infusion of glucose and repeated testing of the blood glucose concentration to avoid excessive hyperglycemia (24).

Carbon-11-methionine is the most intensively studied agent for evaluation of amino-acid metabolism of brain tumors (13,25-28). Preliminary studies showed that ^{11}C -methionine may be superior to FDG in definition of tumor extent and detection of tumor recurrence (25). However, the short half-life of ^{11}C -methionine and other ^{11}C -labeled amino acids restricts the use of these tracers to PET centers with onsite cyclotrons. In contrast, IMT-SPECT offers widespread application of amino acid studies, in that SPECT cameras are generally available and relatively inexpensive. Fluorinated amino acid analogs, such as fluor-tyrosine, which would allow labeling with ^{18}F ($T_{1/2}$ 110 min) have not gained widespread acceptance because of the low radiochemical yield (29).

Both amino-acid and glucose uptake increase markedly after malignant transformation of cells in vitro (30). However, variable quantitative relations between uptake of amino-acids

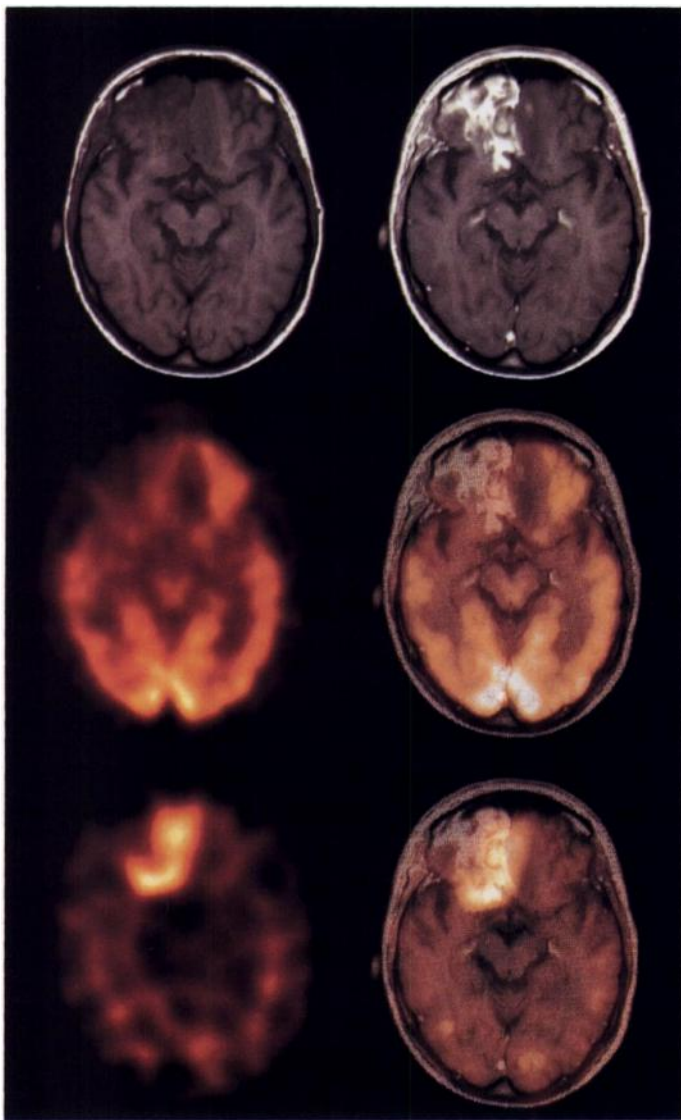


FIGURE 1. T1-weighted MR image before and after administration of Gd-DTPA (first row), FDG-PET (second row), IMT-SPECT (third row) and overlay images of Patient 10 with a recurrent glioblastoma of the left frontal pole. IMT-SPECT shows intense focal IMT uptake at the site of the recurrence. FDG uptake in the tumor is difficult to distinguish from normal gray matter. PET and IMT studies were reorientated using a program developed by Pietrzyk et al. (43) Overlay images were constructed by pixel interleaving (44).

and glucose were observed in different phases of cell growth and in different cell lines (31). A few studies have compared tracers of amino-acid and glucose metabolism in human gliomas: Ericson et al. (32) compared qualitatively the uptake of ^{11}C -glucose and ^{11}C -methionine in 16 patients with supratentorial tumors. They found that six of nine Grade II astrocytomas showed increased uptake of ^{11}C -methionine compared with the normal cortex, whereas none of them were visualized by FDG. Ogawa et al. (25) noticed a high accumulation of ^{11}C -methionine in two recurrent astrocytomas III while FDG uptake in these lesions was low. Wienhard et al. (33) found a weak but still significant correlation between the transport constant K_1 of FDG and ^{18}F -fluorotyrosine in 15 patients with various brain tumors. In our study, we found no significant correlation between IMT and FDG uptake ratios in brain tumors. This may be explained in part by technical differences in the measurement of the tracer uptake (attenuation artifacts in SPECT images and different resolutions of the PET and SPECT scanners). The high uptake of IMT in the two low-grade tumors,

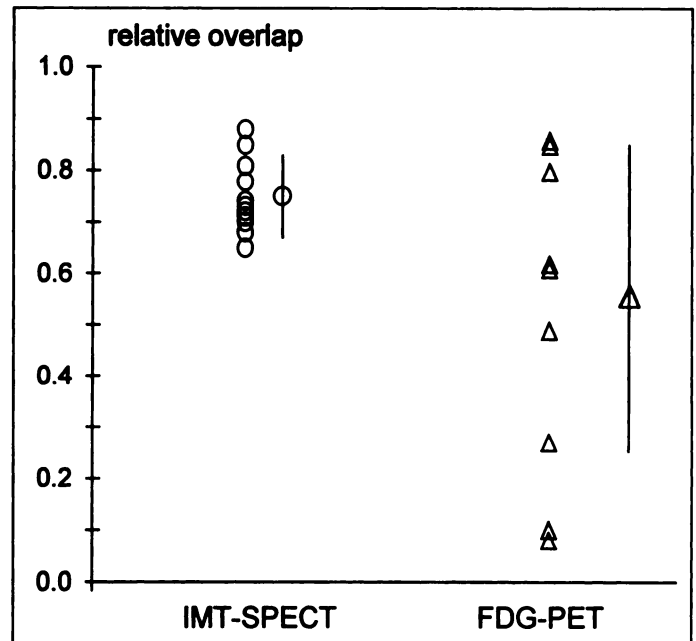


FIGURE 2. Percentage of overlap between the ROIs defined in the IMT-SPECT and FDG-PET studies by the two observers. The percentage of overlap is significantly ($p = 0.03$) higher for IMT-SPECT than for FDG-PET.

as well as some high-grade tumors that showed only low FDG uptake, suggests that despite these technical differences amino acid transport and glucose metabolism in brain tumors are only weakly correlated.

As already observed by the initial investigators of FDG-PET in brain tumors (5,6), we found a significant correlation between histological grading and FDG uptake. In contrast, no correlation was observed between histological grading and IMT uptake in our patients. Similar results were observed with PET tracers of amino acid metabolism. Wienhard et al. (33) found no significant correlation between tumor grading and the influx rate of ^{18}F -tyrosine in 15 patients with various brain tumors. Pruim et al. (34) observed no significant correlation between the protein synthesis rate determined by ^{11}C -tyrosine and histological grading in 22 patients. Nevertheless, in a larger series of patients, a significant correlation between histological grading and IMT uptake may be found. However, it seems unlikely that the correlation would be close enough to allow clinical application of IMT for noninvasive tumor grading.

The high contrast of low-grade as well as high-grade tumors in IMT-SPECT can be advantageous with respect to other possible applications. For low-grade tumors, the definition of tumor extent by CT and MR is difficult due to lacking or only slight contrast enhancement. It is, therefore, often impossible to differentiate tumor tissue and associated edema (4). For these patients, IMT-SPECT could be used for preoperative planning of tumor resection or for defining the target volume for radiotherapy.

The disruption of the blood-brain-barrier by high-grade tumors can be easily visualized by contrast enhancement in CT and MR. The area of enhancement corresponds to the part of the tumor with the highest cell density with only sparse or no intervening normal tissue (35). Increased signal intensities in the T2-weighted MR images clearly delineate brain edema, but tumor may extend beyond the edema. Conversely, not all edematous tissue is infiltrated by tumor cells (35,36). Current radiotherapy strategies therefore include all the edema visible on the T2-weighted images in the radiation field with an additional safety margin of 2 cm (37). In many patients, this

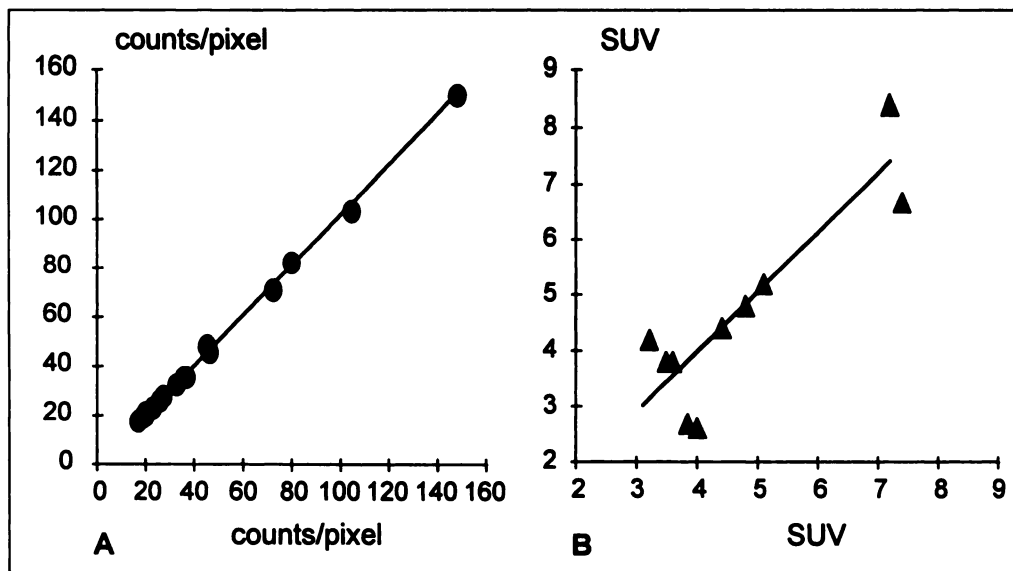


FIGURE 3. (A) Correlation between mean IMT uptake in the ROIs defined by the two observers ($r = 0.999$, $p = 0.0001$). (B) Correlation between mean FDG uptake in the ROIs defined by the two observers ($r = 0.84$, $p = 0.002$).

results in large treatment fields, thus limiting the radiation dose that can be administered without serious side effects (37). A more exact definition of the tumor margins by IMT-SPECT may contribute to improve radiotherapy of brain tumors. Preliminary studies (38) showed that the distribution of IMT uptake in brain tumors closely resembles ^{11}C -methionine uptake, which proved to provide better delineation of tumor infiltration compared to MR and CT (26,27). While IMT-SPECT alone does not provide enough topographical information for planning radiation therapy or stereotactic biopsies, the use of overlay images with CT or MR can make this approach feasible.

With respect to the potential of IMT-SPECT compared to FDG in the differential diagnosis of brain tumors versus benign conditions, the results of this study are clearly limited. Only three patients with nontumorous lesions were investigated and histological confirmation was not obtained in two of them. Therefore, it is not possible to comment on the absolute sensitivity and specificity of IMT-SPECT compared to FDG-PET. However, since these patients had negative PET and SPECT results, the comparison of the two methods is not affected. Furthermore, it is interesting that no increased IMT accumulation was observed, despite intensive contrast enhancement in one patient (no. 18) with radiation necrosis.

Few data are currently available regarding IMT uptake in benign tumors and during the postoperative period. Guth-Tougelidis et al. (39) reported on three patients with suspected

tumor recurrence after surgery and negative IMT scans. In these patients, clinical follow-up (6–24 mo) revealed no evidence of tumor recurrence (39). In our study, a patient with a non-neoplastic hematoma showed only weak, rim-like enhanced IMT uptake. A similar result was obtained by Ogawa et al. (40) who studied four patients with non-neoplastic hematoma with ^{11}C -methionine. The FDG-PET scan of our patient was considered as positive by both observers because of focal FDG accumulation at the periphery of the lesion. Similar increased FDG uptake at the periphery of intracerebral hematomas was previously noted by Dethy et al. (41).

Wagner et al. (42) reported excellent sensitivity of IMT-SPECT in the localization of residual tumor and tumor recurrence after surgery and intraoperative radiotherapy in 20 patients, but they do not give information about the specificity of the method. In our experience, clear more intensive tracer uptake was noted in the area of residual tumor in three patients who had undergone surgery between 1 and 4 wk before IMT-SPECT, whereas the other resection margins showed only weak band-like tracer accumulation. However, these findings have to be confirmed in a larger series of patients at various intervals after surgery.

CONCLUSION

Despite the limited resolution and sensitivity of SPECT compared with PET, IMT-SPECT was clearly superior to

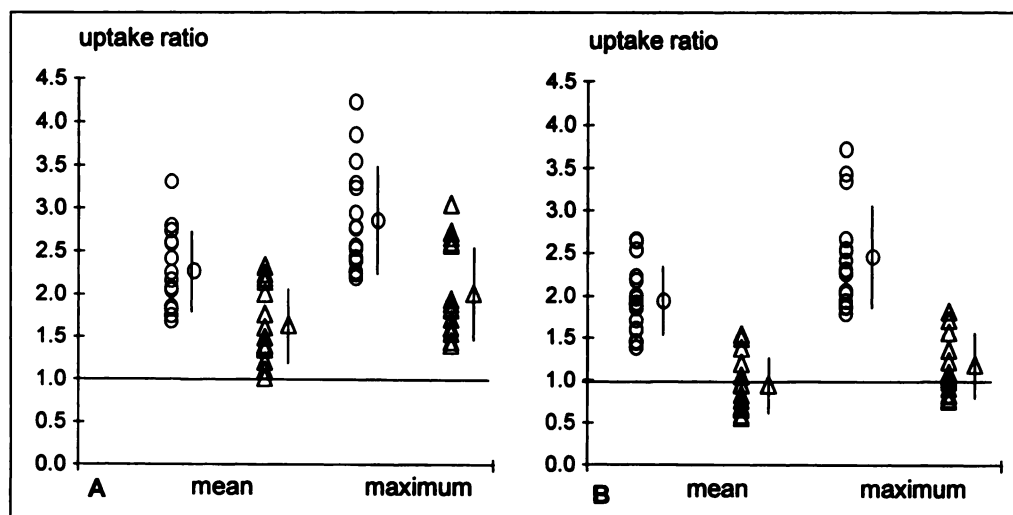


FIGURE 4. Uptake ratios of IMT (circles) and FDG (triangles). (A) Mean and maximum tumor uptake relative to normal white matter. (B) Mean and maximum tumor uptake relative to normal gray matter. All uptake ratios are significantly ($p < 0.001$) higher for IMT than for FDG. The difference between IMT and FDG remains significant even when only glioblastomas were analyzed ($p < 0.01$).

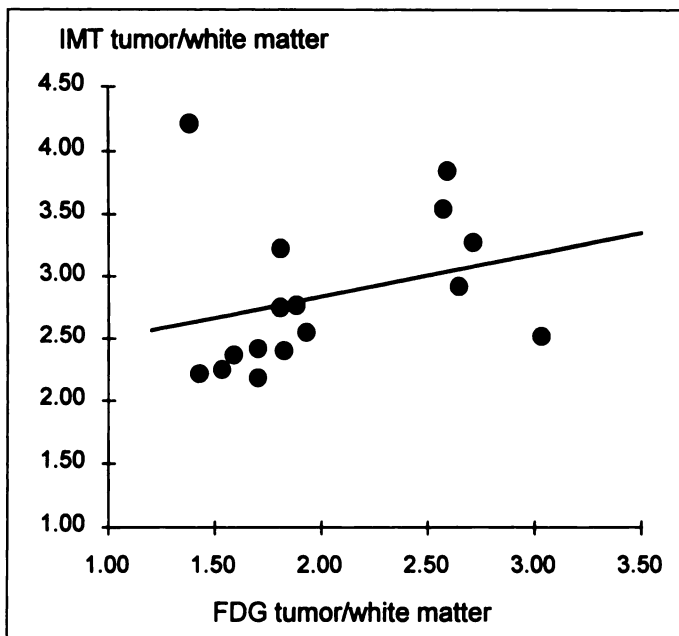


FIGURE 5. Correlation between maximum tumor uptake of FDG and IMT relative to normal white matter ($r = 0.29$, $p = 0.27$).

FDG-PET in the detection and delineation of gliomas. In contrast to FDG-PET, IMT-SPECT seems not to be suitable for noninvasive tumor grading. The high contrast of IMT-SPECT may be useful for planning surgical resections and radiotherapy using overlay images with CT or MR. The specificity of the method appears promising but requires further evaluation in a larger series of patients with benign conditions.

ACKNOWLEDGMENTS

We thank U. Pietrzyk, PhD, Max Plank Institut for Neurology, Cologne, Germany, for generously providing the software package for image correlation. We thank the Department of Nuclear Medicine, University Münster, especially W. Brandau, PhD, for helping to establish the labeling of IMT. We also thank the cyclotron and radiochemistry staff for their contributions and by the technologists in our department for excellent technical support. We also thank Jodi Nerverve for editorial assistance.

REFERENCES

- Blasberg RG. Prediction of brain tumor therapy response by PET. *J Neurooncol* 1994;22:281-286.
- Archibald YM, Lunn D, Lesley AR, et al. Cognitive functioning in long-term survivors of high-grade glioma. *J Neurosurg* 1994;80:247-253.
- Salzman M, Scholtz H, Kaplan RS, Kulik S. Long-term survival in patients with malignant astrocytoma. *Neurosurgery* 1994;34:213-219.
- Sartor K. Tumors and related conditions. In: Sartor K, ed. *MR imaging of the skull and brain: a correlative text-atlas*, 1st ed. Berlin: Springer; 1992:249-493.
- Di Chiro G, De La Paz RL, Brooks RA, et al. Glucose utilization of cerebral gliomas measured by ^{18}F -fluorodeoxyglucose and positron emission tomography. *Neurology* 1982;32:1323-1329.
- Di Chiro G. Positron emission tomography using [^{18}F]fluorodeoxyglucose in brain tumors: a powerful and prognostic tool. *Invest Radiol* 1986;22:360-371.
- Alavi JB, Alavi A, Chawluk J, et al. Positron emission tomography in patients with glioma: a predictor of prognosis. *Cancer* 1988;62:1074-1078.
- Glantz MJ, Hoffman JM, Coleman RE, et al. Identification of early recurrence of primary central nervous system tumors by [^{18}F]fluorodeoxyglucose positron emission tomography. *Ann Neurol* 1991;29:347-355.
- Tyler JL, Diksic M, Villemure JG, et al. Metabolic and hemodynamic evaluation of gliomas using positron emission tomography. *J Nucl Med* 1987;28:1123-1133.
- Janus TJ, Kim EE, Tilbury R, Bruner JM, Yung WK. Use of [^{18}F]fluorodeoxyglucose positron emission tomography in patients with primary malignant brain tumors. *Ann Neurol* 1993;33:540-548.
- Kahn D, Follett KA, Bushnell DL, Nathan MA, et al. Diagnosis of recurrent brain tumor: value of ^{201}Tl SPECT versus ^{18}F -fluorodeoxyglucose PET. *Am J Roentgenol* 1994;163:1459-1465.
- Hawkins RA, Huang SC, Barrio JR, et al. Estimation of local cerebral protein synthesis rate with L-[^{1-14}C]leucine and PET: methods, model and results in animals and humans. *J Cereb Blood Flow Metab* 1989;9:446-460.

- Schober O, Meyer GJ, Duden C, et al. Die Aufnahme von Aminosäuren in Hirntumoren mit der Positronen-Emissionstomographie als Indikator für die Beurteilung von Stoffwechsellaktivität und Malignität. *Fortschr Geb Röntgenstr Nuklearmed* 1987;147:503-509.
- Kloss G, Leven M. Accumulation of radioiodinated tyrosine derivatives in adrenal medulla and in melanomas. *Eur J Nucl Med* 1979;4:179-186.
- Langen KJ, Coenen HH, Roosen N, et al. SPECT studies of brain tumors with L-3-[^{123}I]iodo-alpha-methyl tyrosine: comparison with PET, ^{124}I -IMT and first clinical results. *J Nucl Med* 1990;31:281-286.
- Kawai K, Fujibayashi Y, Saji H, et al. A strategy for the study of cerebral amino acid transport using iodine-123-labeled radiopharmaceutical: 3-iodo-alpha-methyl-L-tyrosine. *J Nucl Med* 1991;32:819-824.
- Langen KJ, Roosen N, Coenen HH, et al. Brain and brain tumor uptake of L-3[^{123}I]iodo-alpha-methyl tyrosine: competition with natural L-amino-acids. *J Nucl Med* 1991;32:1225-1228.
- Biersack HJ, Coenen HH, Stöcklin G, et al. Imaging of brain tumors with L-3-[^{123}I]iodo-alpha-methyl tyrosine and SPECT. *J Nucl Med* 1989;30:110-112.
- Hamacher K, Coenen HH, Stöcklin G. Efficient stereospecific synthesis of non-carrier-added 2-F-18-fluoro-2-deoxy-D-glucose using aminopolyether supported nucleophilic substitution. *J Nucl Med* 1986;27:235-238.
- Krummeich C, Holschbach M, Stöcklin G. Direct n.c.a. electrophilic radiation of tyrosine analogues: their in vivo stability and brain uptake in mice. *Appl Radiat Isot* 1994;45:929-935.
- Münzing W, Raithel E, Tatsch K, Hahn K. Entwurf eines speziellen Kollimators für J-123 und erste Erfahrungen bei der Anwendung [Abstract]. *Nuklearmedizin* 1996;35: A48.
- Cohen J. A coefficient of agreement for nominal scales. *Educ Psychol Meas* 1960;20:37-46.
- Delbeke D, Meyerowitz CM, Lapdus RL, et al. Optimal cutoff levels of F-18-fluorodeoxyglucose uptake in the differentiation of low-grade from high-grade brain tumors with PET. *Radiology* 1995;195:47-52.
- Ishizu K, Nishizawa S, Yonekura Y, et al. Effects of hyperglycemia on FDG uptake in human brain and glioma. *J Nucl Med* 1994;35:1104-1109.
- Ogawa T, Kanno I, Shishido F, et al. Clinical value of PET with F-18-fluorodeoxyglucose and L-methyl-C-11-methionine for diagnosis of recurrent brain tumor and radiation injury. *Acta Radiol* 1991;32:197-202.
- Moskinn M, Ericson K, Hindmarsh T, et al. PET compared with MRI and CT in supratentorial gliomas using multiple stereotactic biopsies as a reference. *Acta Radiol* 1989;30:225-232.
- Tovi M, Lilja A, Bergstroem M, Ericsson A, Bergstroem K, Hartman M. Delineation of gliomas with magnetic resonance imaging using Gd-DTPA in comparison with computed tomography and positron emission tomography. *Acta Radiol* 1990;31:417-429.
- Ogawa T, Shishido F, Kanno I, et al. Cerebral glioma: evaluation with methionine PET. *Radiology* 1993;186:45-53.
- Lemaire C. Production of L-F-18-fluoro amino acids for protein synthesis: overview and recent developments in nucleophilic syntheses. In: Mazoyer BM, Heiss WD, Comar D, eds. *PET studies of amino acid metabolism and protein synthesis*. Dordrecht: Kluwer Academic Publishers; 1993:89-108.
- Isselbacher KJ. Increased uptake of amino acids and 2-deoxy-D-glucose by virus-transformed cells in culture. *Proc Nat Acad Sci USA* 1972;69:585-589.
- Minn H, Clavo AC, Grenman R, Wahl RL. In vitro comparison of cell proliferation kinetics and uptake of fluorodeoxyglucose and L-methionine in squamous-cell carcinoma of the head and neck. *J Nucl Med* 1995;36:252-258.
- Ericson K, Lilja A, Bergström M, et al. Positron emission tomography with C-11-L-methionine, C-11-D-glucose and Ga-68-EDTA in supratentorial tumors. *J Comput Assist Tomogr* 1985;9:683-689.
- Wienhard K, Herholz K, Coenen HH, et al. Increased amino acid transport into brain tumors measured by PET of L-2-F-18-fluorotyrosine. *J Nucl Med* 1991;32:1338-1346.
- Pruim J, Willemsen ATM, Molenaar, WM, et al. Brain tumors: L-1-C-11-tyrosine PET for visualization and quantification of protein synthesis rate. *Radiology* 1995;197:221-226.
- Earnest F, Kelly PJ, Scheithauer BW, et al. Cerebral astrocytomas: histopathological correlation of MR and CT contrast enhancement with stereotactic biopsy. *Radiology* 1988;166:823-827.
- Kelly PJ, Daumas-Duport C, Kispert DB, et al. Imaging-based stereotactic serial biopsies in untreated intracranial glial neoplasms. *J Neurosurg* 1987;66:865-874.
- Karson UL, Leibel SA, Wallner K, Davis LW, Brady LW. Brain. In: Perez CA, Brady LW, eds. *Principles and practice of radiation oncology*, 2nd ed. Philadelphia: JB Lippincott; 1992:515-563.
- Langen KJ, Csaplar K, Ziemons K, et al. Studies of amino acid uptake in gliomas with ^{123}I -alpha-L-methyltyrosine: comparison with ^{14}C -L-methionine in vitro and in vivo [Abstract]. *J Cereb Blood Flow Metab* 1995;15(suppl):S172.
- Guth-Tougelidis B, Müller S, Mehndorn MM, et al. Anreicherung von DL-3- ^{123}I -alpha-methyltyrosin in hirntumorzidiven. *Nuklearmedizin* 1995;34:71-75.
- Ogawa T, Hatazawa J, Atsushi I, et al. Carbon-11-methionine PET evaluation of intracerebral hematoma: distinguishing neoplastic from non-neoplastic hematoma. *J Nucl Med* 1995;36:2175-2179.
- Dethy S, Goldman S, Bleccic S, et al. Carbon-11-methionine and ^{18}F fluorine-FDG-PET study in brain hematoma. *J Nucl Med* 1994;35:1162-1166.
- Wagner W, Schuller P, Willich N, et al. Intraoperative Strahlentherapie (IORT) malignen Hirntumoren. *Strahlenther Onkol* 1995;17:154-164.
- Pietrzyk U, Herholz K, Fink G, et al. An interactive technique for three-dimensional image registration: validation for PET, SPECT, MRI and CT brain studies. *J Nucl Med* 1994;35:2011-2018.
- Rehm K, Strother SC, Anderson JR, Schaper KA, Rottenberg DA. Display of merged multimodality brain images using interleaved pixels with independent color scales. *J Nucl Med* 1994;35:1815-1821.